

1 Hammersley's process

In the previous lecture we defined Hammersley's process:

1. particles occupy points on \mathbb{R}
2. ω is a Poisson point process on \mathbb{R}^2 (space-time)
3. if $(x, t) \in \omega$ then at time t the particle closest to x among those to the left of x moves to x

In this lecture we will discuss a connection between the Hammersley's process and maximal increasing subsequences in random permutations, and then investigate an interplay between the dynamics of Hammersley's process and multi-type TASEP dynamics.

1.1 Some preliminaries

Before we explain an interesting connection between Hammersley's process and permutations, we review some classical results on permutations. For more details, refer to e.g. [Sag01].

A *Ferrers diagram* is a finite array with left-justified rows of weakly decreasing lengths.

A *standard Young tableau (SYT)* of size n and shape $\xi_1 \geq \xi_2 \geq \dots \geq \xi_\ell$ is a filling of a Ferrers diagram with row lengths $\xi_1, \xi_2, \dots, \xi_\ell$ with the numbers $1, 2, \dots, n$ so that each column, as read from top to bottom, and each row, as read from left to right, is an increasing subsequence of $(1, 2, \dots, n)$ (we require $\sum \xi_i = n$).

The *Robinson-Schensted algorithm (RSA)* provides a bijection between the symmetric group \mathcal{S}_n and pairs of standard Young tableaux of the same shape and of size n . Simply put, the RSA takes in a permutation

$$\begin{pmatrix} 1 & 2 & \cdots & n \\ \pi_1 & \pi_2 & \cdots & \pi_n \end{pmatrix}$$

and, after n iterations, returns a pair (P_π, Q_π) of SYT of the same shape and of size n . Each iteration of RSA returns a pair of tableaux (P^k, Q^k) , each of size k . The i th iteration consists of adding π_i to the end of the first row of P^{i-1} if π_i is larger than all elements of the row; or else replacing the least element, x say, in the row which is greater than π_i with π_i and then adding x to P^{i-1} less its first row by the same method. In whatever position this process terminates — thus forming P^i — we place an i in the corresponding entry in Q^{i-1} to form Q^i . We define $(P_\pi, Q_\pi) = (P^n, Q^n)$. For example, see Figure 1.

i	0	1	2	3	4	5
P^i	\emptyset	3	1 3	1 2 3	1 2 5 3	1 2 4 3 5
Q^i	\emptyset	1	1 2	1 3 2	1 3 4 2	1 3 4 2 5

Figure 1: RSA with input $\pi = 31254$.

By carefully analysing RSA, we see that the pair (P_π, Q_π) encodes some important information about π . For instance, the length of the first row (column) of P_π (and Q_π) is equal to the length of maximal increasing (decreasing) subsequences of π .

Viennot's geometric construction [Vie77] of the RSA yields an elegant proof of the fact $\pi \xrightarrow{\text{RS}} (P, Q)$ if and only if $\pi^{-1} \xrightarrow{\text{RS}} (Q, P)$ (cf. [Sch63]). For a permutation $\pi \in \mathcal{S}_n$ we define the i th shadow box of π as

$$\mathfrak{B}_i = \{(x, y) \in \mathbb{R}^2 : x \geq i, y \geq \pi(i)\}.$$

For example, the third shadow box for $\pi = 31254$ appears in Figure 2.

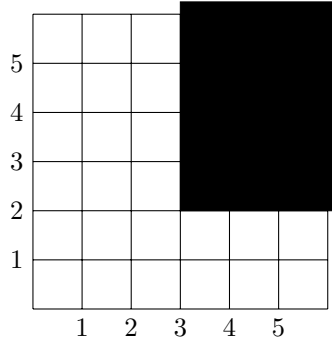


Figure 2: \mathfrak{B}_3 for $\pi = 31254$

The shadow lines of $\pi \in \mathcal{S}_n$ are built recursively:

$$\mathfrak{L}_1 = \partial \bigcup_{i \in \mathfrak{I}_1} \mathfrak{B}_i$$

$$\mathfrak{L}_j = \partial \bigcup_{i \in \mathfrak{I}_j} \mathfrak{B}_i, \quad 1 < j \leq k$$

where

$$\mathfrak{I}_1 = \{1, 2, \dots, n\}$$

$$\mathfrak{I}_j = \left\{ q : (q, \pi(q)) \cap \bigcup_{i=1}^{j-1} \mathfrak{L}_i = \emptyset \right\}, \quad 1 < j < k,$$

k is the smallest integer so that

$$\{1, 2, \dots, n\} \subset \bigcup_{i=1}^k \mathfrak{L}_i$$

and ∂A denotes the boundary of a set A .

For example, the permutation $\pi = 31254$ has three shadow lines; as seen in Figure 3.

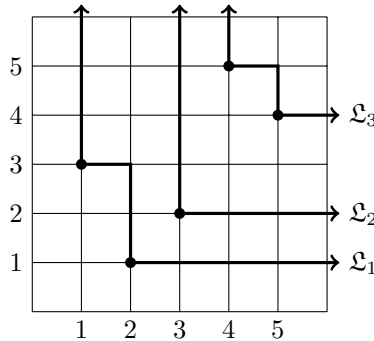


Figure 3: Shadow lines for $\pi = 31254$.

Observe that in Figure 3, the vertical rays point towards the first row of P_π , and the horizontal rays point towards the first row of Q_π . This is no coincidence, and is indeed, precisely what Viennot proved (*Hint*: Every vertical cut along an integer in the shadow line display intersects a shadow line at a point, finite line segment, or vertical ray. Every step of RSA either places an integer at the end of the first row or displaces an element of the first row. Likewise, each element of the first row is either displaced or its position is maintained.) Moreover, the entire tableaux pair (P_π, Q_π) can be recovered by this geometric method. To acquire the i th rows we perform the shadow box procedure on the partial permutation defined by the upper corners (dual points) in the $(i-1)$ th set of shadow lines. See Figure 4. Viennot completes the proof by simply reflecting in the line $y = x$ and repeating his procedure one last time. Incredible!

1.2 Maximal increasing subsequences and Hammersely's process

To see a connection between Hammersely's process and maximal increasing subsequences in random permutations, consider the following situation. We begin with an infinite stack of particles at the origin (with priority given to particles closest to the axis), then plot the configuration evolution in space and time as in Figure 5. The open circles denote events $(x, t) \in \omega$, the dotted polygonal paths track the position of particles in time, and the closed circles below display the configuration at time t_0 .

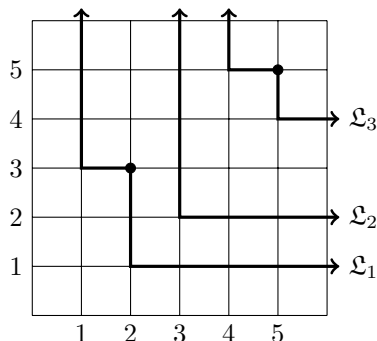


Figure 4: The upper corners (dual points) of first set of shadow lines of $\pi = 31254$ are $(2, 3)$ and $(5, 5)$. Hence to get the second rows of (P_π, Q_π) we repeat the shadow line procedure on the partial permutation π_2 defined by $\pi_2(2) = 3$ and $\pi_2(5) = 5$.

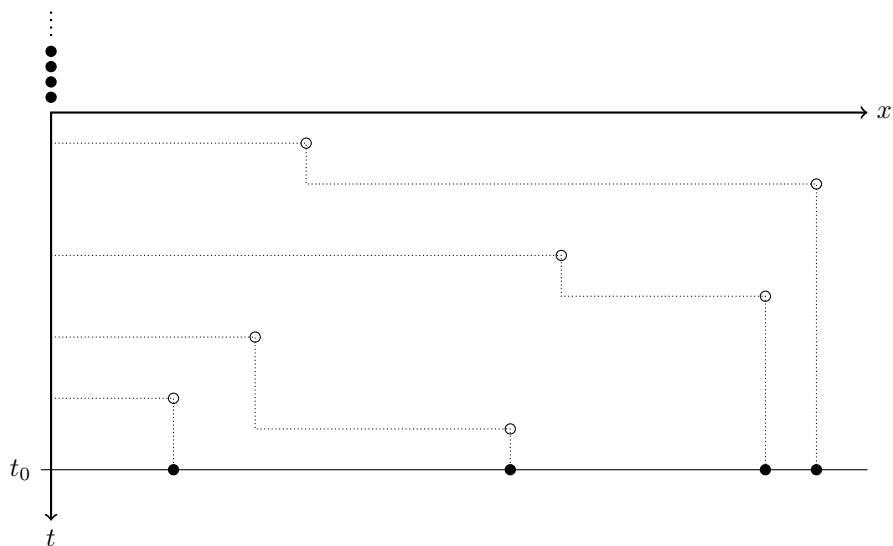


Figure 5: Graphical representation of Hammersely's process with stack initial conditions.

The events in ω up to a given time (i.e. the open circles as in Figure 5) can be viewed as a representation for a permutation. Suppose k events have occurred up to time t_0 :

$$(x_1, t_1), (x_2, t_2), \dots, (x_k, t_k)$$

where $x_i > x_{i+1} > 0$ and $0 < t_i \leq t_0$ for all i . For each i , let $\phi(t_i) = \ell$ if t_i is the

ℓ th smallest of the t_j . Then, to this sequence of events, assign the permutation

$$\begin{pmatrix} 1 & 2 & \cdots & k \\ \phi(t_1) & \phi(t_2) & \cdots & \phi(t_k) \end{pmatrix}.$$

For example, the events up to time t_0 in Figure 5 correspond to the permutation

$$\sigma = \begin{pmatrix} 1 & 2 & 3 & 4 & 5 & 6 & 7 \\ 2 & 4 & 3 & 7 & 1 & 5 & 6 \end{pmatrix}.$$

Notice that if we rotate Figure 5 by 180° the dotted lines coincide with the (first set of) shadow lines for the permutation σ in Viennot's geometric construction of RSA, as discussed in the previous subsection. Therein we observed that the number of vertical rays in the first set of shadow lines of a permutation is equal to the maximal length of increasing subsequences of the permutation. Hence, we see that if k events in ω have occurred up to time t_0 , then the number of particles in Hammersely's process (with the initial conditions described above) at time t_0 is equal to the maximal length of increasing subsequences in a random permutation of \mathcal{S}_k .

Exploiting this connection Aldous and Diaconis [AD95] showed that

$$\lim_{n \rightarrow \infty} n^{-1/2} \mathbf{E}L_n = 2$$

where L_n is the maximal length of increasing subsequences in a uniformly selected permutation of \mathcal{S}_n (cf. [KV77], [LS77]).

1.3 Basic coupling of Hammersely processes and multi-type TASEP dynamics

For details regarding the remainder to today's notes, refer to [Ang06] and [FM07].

To apply the basic coupling, under the Hammersely's process dynamics, to a pair of configurations, one contained in the other, we can once again make use of first and second particles. See Figure 6.

We can generalise the scenario depicted in the middle diagram in Figure 6 as follows: if an event at x occurs directly to the right of a string of the form $122 \cdots 2x$, then after the event the string becomes $222 \cdots 1$. That is, the topmost particle in the 1 and the particle in the rightmost 2 move to x and there form a 1. As a result, the position previously occupied by the rightmost 2 becomes unoccupied and the 1 becomes a 2.

Naturally, we can extend this coupling to any number of lines. A scenario with three lines is depicted in Figure 7. We can generalise the scenario depicted in the figure: if an event at x occurs directly to the right of a string of the form $1\gamma_1\gamma_2 \cdots \gamma_\ell 23 \cdots 33x$, for $\gamma_i \in \{0, 1\}$, then after the event the string becomes $2\gamma_1\gamma_2 \cdots \gamma_\ell 33 \cdots 31$. In words, the topmost particle in the 1, the topmost particle in the rightmost 2, and the particle in the rightmost 3 move to x and there form a 1. Hence, the position previously occupied by the rightmost 3 becomes

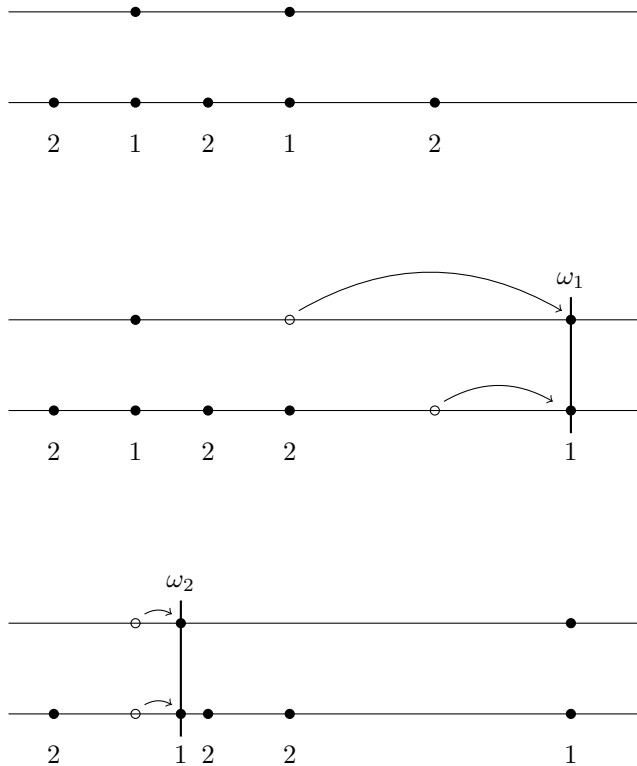


Figure 6: *Top*: Coupled Hammersley processes. *Middle*: Event occurs to right of 12 — as a result: $12 \rightarrow 21$. *Bottom*: Event occurs between 12 — as a result: $12 \rightarrow 12$.

unoccupied, the 1 becomes a 2, and the rightmost 2 becomes a 3. Similarly, we can analyse events of the form $1\gamma_1\gamma_2\cdots\gamma_\ell 2x$.

We conclude this section with an important observation: the basic coupling of Hammersley processes implicitly defines a multi-type TASEP dynamical system.

1.4 Stationary measures for multi-type TASEP

As discussed in the previous lecture, Poisson measures μ_λ with intensity λ are stationary for Hammersley's process. In this subsection we investigate stationary measures for the multi-type TASEP defined in the previous subsection. For this study, a method, known as 'collapsing,' will prove very useful.

Suppose we have two configurations of particles on \mathbb{R} . We can *collapse* these configurations onto each other in the following way: we draw the configurations on top of each other, then connect each particle in the top row to the particle on the bottom row closest to its right. Positions in the bottom row corresponding to

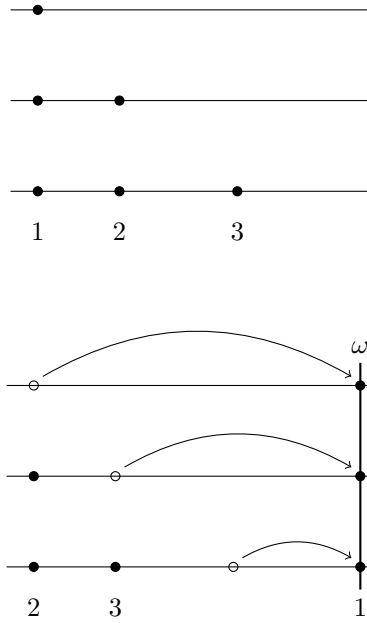


Figure 7: *Top*: Coupling three Hammersely processes. *Bottom*: Event occurs to right of 123 — as a result: $123 \rightarrow 231$.

a connection are labelled 1, and positions corresponding to unconnected particles are labelled 2. See Figure 8. The resulting collapsed configuration has an interpretation as a queue: the particles in the top row can be viewed as customer arrivals and the bottom particles as attempted services. In this interpretation, the collapsing procedure identifies customers with their service times, denoted by 1's, and so 2's denote unused services. Note that, e.g. in Figure 8, the number of intersections of identification lines with a vertical line at t is equal to the number of customers in the queue at time t .

The collapsing procedure can be generalised, in the natural way, to accommodate any number of configurations. Formally, the collapsing procedure sends a point process Ω^k to a k -type process:

$$C : \Omega^k \mapsto \Omega_k.$$

Figure 9 provides an example in the three-dimensional setting. In drawing the connection lines, priority is given to particles which are connected to more particles in rows above. Again, we can interpret the result of the collapsing procedure as the status of a queue in which customers are served in order with respect to how many queues they have departed from in the past.

We are specifically interested in finding a stationary measure for the multi-type TASEP of the following form:

Definition 1. For $0 < \lambda_1 < \lambda_2 < \dots < \lambda_k$, let μ_λ be the stationary measure

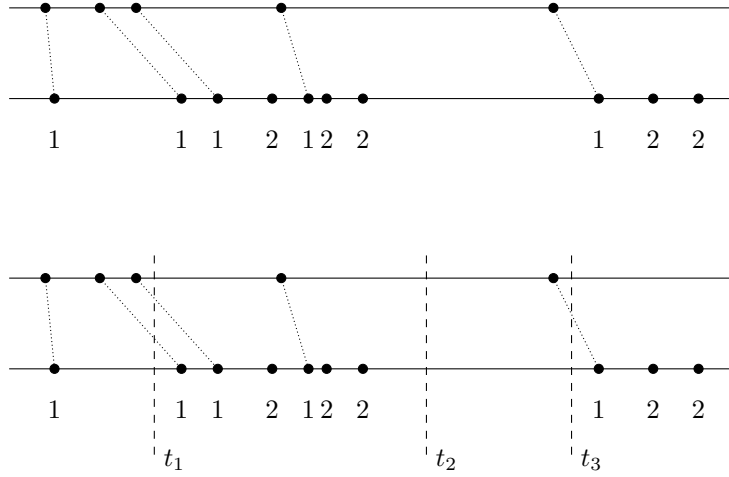


Figure 8: *Top*: Collapsing of two configurations onto a 2-type particle configuration. *Bottom*: Two customers in the queue at time t_1 ; no customers in the queue at time t_2 ; one customer in the queue at time t_3 .

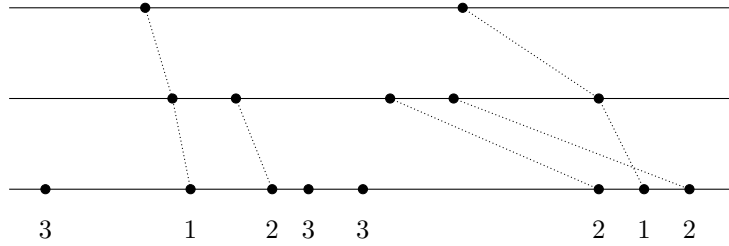


Figure 9: Collapsing of three configurations onto a 3-type particle configuration.

on Ω_k with intensity λ_i for the total number of particles of classes 1 through i . Furthermore, let ν_λ be the product measure on Ω^k where the i th line has intensity λ_i .

As we shall see, the stationary measure μ_λ and the product measure ν_λ satisfy the following relation:

Theorem 2. *With C , μ_λ and ν_λ as defined above:*

$$\mu_\lambda = C \circ \nu_\lambda.$$

Before proving Theorem 2, we look further into the connection between collapsing and the dynamics of Hammersley's process.

Let H_ω be the dynamics of Hammersley's process with ω driving process. Then, given $X_0 \in \Omega_k$, put $X_t = H_{\omega|_{[0,t]}}(X_0)$. The dynamics on a single line induces dynamics for the multi-line system Ω^k : given $(x, t) \in \omega$, the particle in

line k (the bottom line) nearest to and on the left of x , at position x_k say, moves to x . Then the particle nearest to and on the left of x_k in line $k-1$, at position x_{k-1} say, moves to x_k . The rule continues as such until a jump occurs in the first line. Although the rule is defined recursively, we think of the k jumps as occurring simultaneously. See Figure 10.

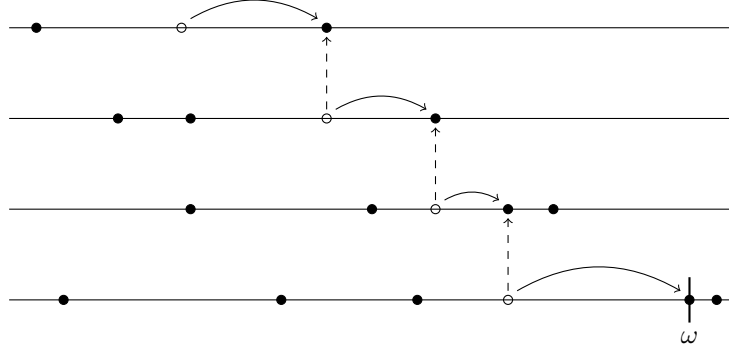


Figure 10: H_ω induced dynamics on Ω^4 .

As we shall see, the action of collapsing commutes with the dynamics of Hammersely's process. This fact plays a significant role in the proof of Theorem 2 below. In Figures 10 and 11 we verify one particular case.

Lemma 3. *With C and H_ω as defined above:*

$$C \circ H_\omega = H_\omega \circ C.$$

Proof. We prove the result by induction on the number of lines (number of types).

Consider the base case with two lines. There are (essentially) two cases to be checked. We verify the statement of the theorem for these cases in Figure 12. Technically there are other cases to consider, but in all cases the proofs are very similar. All cases rely on the fact that in the collapsing procedure, particles in the top row are matched with particles in the bottom row immediately to their right.

To complete the proof, we assume the statement holds for systems with up to $k-1$ lines. Then, to verify the result for a system with k lines we can apply the inductive hypothesis for the bottom $k-1$ lines and then apply the base case to add in the first line (maintaining labels of 1 for particles in the bottom row corresponding to connection lines involved in this addition, and decreasing labels of all particles corresponding to uninvolved connection lines). \square

Having established Lemma 3, we shall easily deduce Theorem 2 after making the following observation:

Lemma 4. *ν_λ is stationary for the multi-line dynamics, as defined above, on Ω^k . In other words, the multi-line dynamics preserve the product measure.*

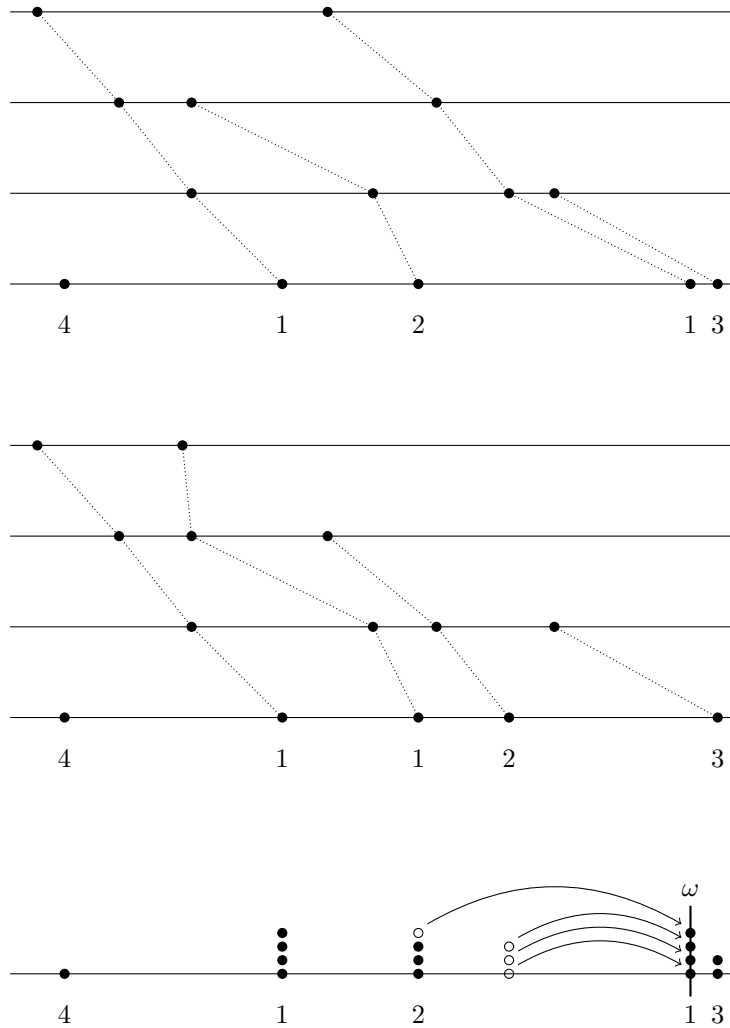


Figure 11: (cf. Figure 10) *Top:* Collapsing after Hammersely dynamics, i.e. $C \circ H_\omega$. *Middle:* Collapsing before Hammersely dynamics. *Bottom:* Hammersely dynamics after collapsing, i.e. $H_\omega \circ C$. *Note:* $C \circ H_\omega = H_\omega \circ C$.

Proof. Recall from the previous lecture that if ω is a Poisson point process, then the set of dual points (open circles in diagrams)

$$\hat{\omega} = \{(x, t) : \text{a particle jumps from } x \text{ at time } t\}$$

is again a Poisson point process: $\hat{\omega} =_d \omega$. This follows from considering the time-space reversal on any finite time interval.

Hence, by induction, we see that each line in the multi-line dynamics is driven by a Poisson point process.

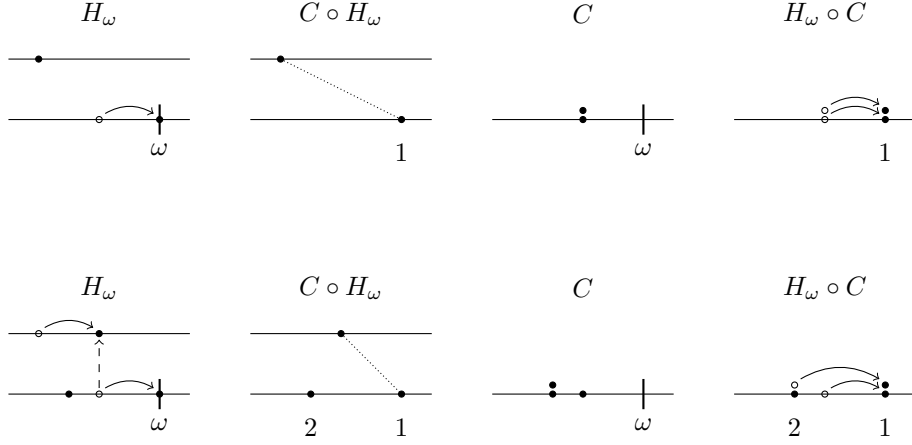


Figure 12: Base cases for inductive proof of Lemma 3.

Moreover, up to any time t the driving process of dual points is independent of the initial configuration on line k (the bottom line). Therefore at time t we still have independence between lines. \square

Finally, we are in a position to prove Theorem 2.

Proof. (of Theorem 2) The multi-type process Ω_k is a collapsed multi-line process. Hence, by Lemmas 3 and 4, we see that $C \circ \nu_\lambda$ is stationary for Ω_k :

$$H_\omega(C \circ \nu_\lambda) = (H_\omega \circ C)(\nu_\lambda) = (C \circ H_\omega)(\nu_\lambda) = C \circ \nu_\lambda.$$

The fact that $C \circ \nu_\lambda$ has intensity λ_i for the total number of particles of classes 1 through i , for all $1 \leq i \leq k$, is evident by the very nature of the collapsing procedure. Hence $C \circ \nu_\lambda = \mu_\lambda$. \square

1.5 Discrete collapsing

Discrete analogues for the results in the previous subsection can be obtained. The results and proof methods are distinct in some respects. For example, in the discrete setting some attempted particle jumps need to be suppressed if there is a particle in an adjacent position. This leads to several different natural choices for couplings of processes.

Some details will be given in the next lecture.

References

- [AD95] Aldous, D.; Diaconis, P. Hammersley's interacting particle process and longest increasing subsequences. *Probab. Theory Related Fields* 103 (1995), no. 2, 199213.

- [Ang06] Angel, O., The stationary measure of a 2-type totally asymmetric exclusion process. *J. Combin. Theory Ser. A* 113 (2006), no. 4, 625635.
- [FM07] Ferrari, P.; Martin, J., Stationary distributions of multi-type totally asymmetric exclusion processes. *Ann. Probab.* 35 (2007), no. 3, 807832.
- [KV77] Kerov, S.; Vershik, A. Asymptotics of the Plancherel measure of the symmetric group and the limiting form of Young tables. *Soviet Math. Dokl.*, 18:527–531, 1977. Translation of Dokl. Acad. Nauk. SSSR 233 (1977) 1024-1027.
- [LS77] Logan, B.; Shepp, L. A variational problem for random Young tableaux. *Advances in Math.*, 26:206-222, 1977.
- [Sag01] Sagan, B., The symmetric group. Representations, combinatorial algorithms, and symmetric functions. Second edition. Graduate Texts in Mathematics, 203. *Springer-Verlag, New York*, 2001.
- [Sch63] Schützenberger, M., Quelques remarques sur une construction de Schensted, *Math Scand.* 12 (1963), 117-128.
- [Vie77] Viennot, G., Une forme gomtrique de la correspondance de Robinson-Schensted, in Cominatorie et Reprsentation du Groupe Symtrique, D. Foata ed., Lecture notes in Math., Vol. 579, *Springer-Verlag, New York, NY*, 1977, 29-58.